Acta Crystallographica Section F
Structural Biology and Crystallization Communications
ISSN 1744-3091

Expression, crystallization and preliminary X-ray analysis of a ferric binding protein from *Thermus thermophilus* HB8

Qing Wang,[a,b] Liying Chang,[a] Xinquan Wang[b] and Xiaoqing Liu[a]*

[a]College of Life Sciences, Capital Normal University, Beijing 100048, People's Republic of China, and [b]Center for Structural Biology, School of Life Sciences, Ministry of Education Key Laboratory of Bioinformatics, Tsinghua University, Beijing 100084, People's Republic of China

Correspondence e-mail: liuxq@mail.cnu.edu.cn

Received 2 March 2011
Accepted 6 April 2011

A ferric binding protein from *Thermus thermophilus* HB8 (TtFbpA) was expressed, purified and crystallized using the hanging-drop vapour-diffusion method. Four different crystal forms were obtained and characterized by X-ray diffraction. Two crystal forms with TtFbpA in the apo state belonged to the orthorhombic space group $P2_12_12_1$ (unit-cell parameters a = 42.1, b = 139.3, c = 326.5 Å and a = 42.1, b = 139.3, c = 218.9 Å). The third form with TtFbpA also in the apo state belonged to the monoclinic space group $P2_1$ (unit-cell parameters a = 66.5, b = 61.7, c = 73.9 Å, β = 111.7°). The fourth form, with TtFbpA in the iron-bound holo state as confirmed by an atomic absorption spectrophotometry assay, belonged to the trigonal space group $P3_121$ or $P3_221$ (unit-cell parameters a = 63.6, b = 63.6, c = 266.7 Å, $\alpha = \beta$ = 90.0, γ = 120.0°).

1. Introduction

Iron is essential to most biological systems as a consequence of its various roles in the biochemistry of living organisms (Higgins, 1992). A variety of mechanisms for iron uptake, transport and storage have been described (Clarke *et al.*, 2001). In Gram-negative bacteria, the soluble ferric ion-binding protein (FbpA) plays an essential role in iron transport by binding ferric ion with high affinity in the periplasm and shuttling it to an ATP-binding cassette (ABC) type importer consisting of FbpB in the inner membrane and the ATPase FbpC in the cytoplasm. The energy for this transport is provided by hydrolysis of ATP (Higgins, 2001).

To help understand the mechanisms of ferric ion loading and removal, structures of FbpA in various states have been studied using X-ray crystallography and extended X-ray absorption fine-structure methods (Bruns *et al.*, 2001; Tom-Yew *et al.*, 2005; Guo *et al.*, 2003; Shouldice *et al.*, 2005; Badarau *et al.*, 2008). These structures display an almost identical overall topology. They are composed of N- and C-domains which are connected by two short strands as a hinge, with the ligand-binding site buried between the two domains (Biemans-Oldehinkel *et al.*, 2006). Anion-dependent ferric binding proteins have been postulated to exist in four distinct structural states, (i) open unliganded, (ii) closed unliganded, (iii) closed liganded and (iv) open liganded; this has been named the 'Venus flytrap' mechanism of ferric ion loading and removal (Berntsson *et al.*, 2010; Mao *et al.*, 1982).

Structures of apo/holo FbpA from several different bacterial strains have been determined, but the observed state was partially influenced by the iron or anion additive used during purification and crystallization. Currently, comparisons of different structural states are only available for FbpA from *Mannheimia haemolytica* in three states (Shouldice *et al.*, 2004) and for hFbp from *Haemophilus influenzae* (Bruns *et al.*, 2001) and FutA2 from *Synechocystis* 6803 (Badarau *et al.*, 2008) in two states. Structural studies of FbpA in all four different states from the same bacterial strain are still needed to facilitate complete understanding of the iron-loading and removal mechanism. The gene TTHA1628 (http://www.srg.harima.riken.jp/h_db/index.html) from *Thermus thermophilus* HB8 encodes a ferric binding protein (TtFbpA) with a molecular weight of 36.1 kDa (residues 1–330) and a calculated isoelectric point of 9.4. Here, the

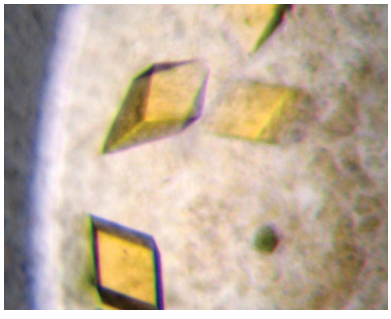

purification, crystallization and preliminary X-ray analysis of TtFbpA in four different crystal forms are reported.

2. Methods and results

2.1. Cloning, expression and purification

TTHA1628 from *T. thermophilus* HB8 was PCR-amplified using the forward primer 5′-AACT**GGATCC**ATGATGAAGCGCTACCT-3′ and the reverse primer 5′-AATA**AGATCT**GAGGACCCCGGTC-TCC-3′ (restriction sites are shown in bold). The PCR product was digested with *Bam*HI and *Bgl*II and ligated into the expression vector pQE70 (Qiagen) containing a His tag at the C-terminus. The plasmid was transformed into *Escherichia coli* DH5α and positive colonies were subsequently selected on ampicillin plates and confirmed by DNA sequencing.

The protein was expressed in *E. coli* XL-1 Blue cells at 310 K in Luria–Bertani (LB) medium supplemented with 100 µg ml^{-1} ampicillin. At an OD_{600} of 0.6–0.8, expression of TtFbpA was induced by addition of isopropyl β-D-1-thiogalactopyranoside (IPTG) to a final concentration of 0.5 m*M*. After further incubation at 303 K for 6 h, the cells were pelleted and resuspended in lysis buffer (10 m*M* HEPES pH 7.2, 150 m*M* NaCl, 10 m*M* imidazole). The collected cells were sonicated and the debris was removed by centrifugation at 15 000 rev min^{-1} at 277 K for 1 h. The supernatant containing His-tagged TtFbpA was loaded onto a HisTrap column (GE Healthcare) and the column was washed extensively with wash buffer (10 m*M* HEPES pH 7.2, 150 m*M* NaCl, 40 m*M* imidazole). The bound His-tagged TtFbpA was eluted with elution buffer (10 m*M* HEPES pH 7.2, 150 m*M* NaCl, 250 m*M* imidazole). The eluate containing TtFbpA was further purified using a Superdex 200 10/300 GL gel-filtration column (GE Healthcare; Fig. 1*a*) and the purity was examined by SDS–PAGE (Fig. 1*b*). TtFbpA was finally concentrated to 20 mg ml^{-1} in 10 m*M* HEPES pH 7.2 and 150 m*M* NaCl using an Amicon Ultra centrifugal filter device (Millipore). The protein concentration was determined using a Nanovue Plus spectrophotometer (GE Healthcare) with an extinction coefficient of 0.92 (one absorbance unit corresponds to 0.92 mg ml^{-1}, as predicted by *Vector NTI* v.7 software).

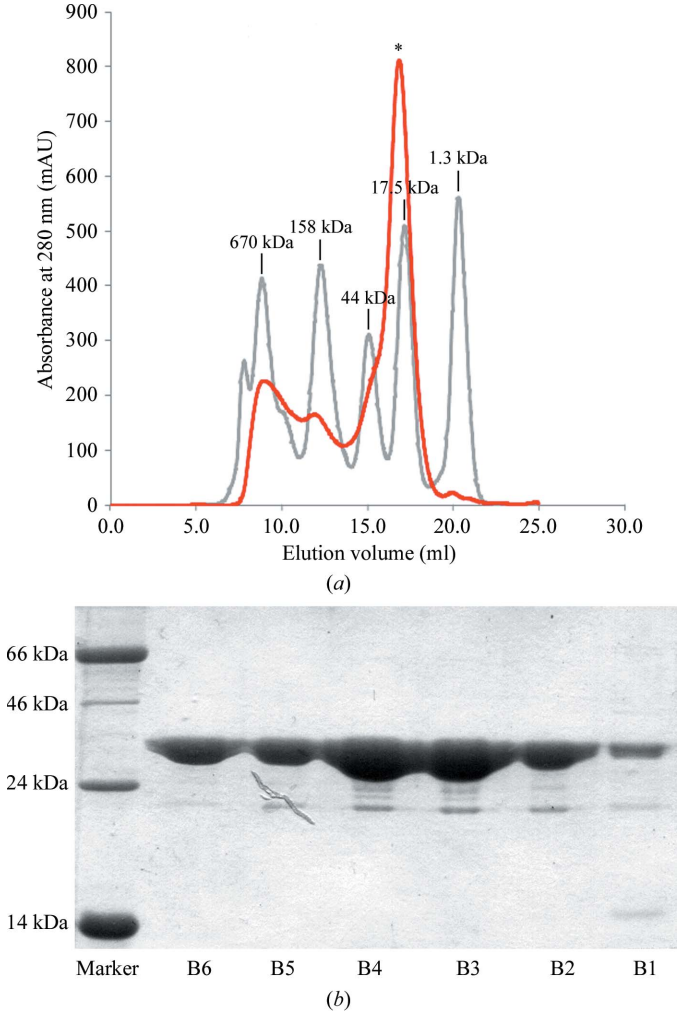

Figure 1
Purification of TtFbpA. (*a*) Elution profile of TtFbpA (red line) by gel-filtration chromatography using a Superdex 200 10/300 GL column. The elution was standardized using a mixture from Bio-Rad. The TtFbpA peak is marked with an asterisk. (*b*) SDS–PAGE analysis of TtFbpA peak fractions from gel filtration, showing the homogeneity of TtFbpA immediately prior to crystallization. Fractions B6–B1 correspond to elution volumes from 15.7 to 18.7 ml, with each fraction consisting of 0.5 ml. The protein ran to its true size of 36.1 kDa upon denaturation.

Table 1
AAS data collection.

Metal ion	Content† (ng g^{-1})
Fe^{2+}/Fe^{3+}	2904.7 ± 164.3
Mn^{2+}	12.7 ± 5.1
Cu^{2+}	81.4 ± 15.7
Zn^{2+}	123.4 ± 3.2
Mg^{2+}	705.9 ± 23.2
Co^{2+}	ND
Ni^{2+}	ND

† Metal content per gram of TtFbpA protein. ND: the metal content is below the detection limit.

2.2. Atomic absorption spectrophotometry

An atomic absorption spectrophotometry (AAS) experiment was conducted to confirm the binding of ferric ion in the orange TtFbpA sample purified with bicarbonate. Three independent AAS measurements were performed at Tsinghua Analysis Centre using a Carl Zeiss Technology Analytic Jena AAS 6 Vario instrument. The sample was analyzed for the presence of the metal ions Mg^{2+}, Mn^{2+}, Fe^{2+}/Fe^{3+}, Co^{2+}, Ni^{2+}, Cu^{2+} and Zn^{2+}. The results indicated that abundant Fe^{2+}/Fe^{3+} remained in the protein solution after gel-filtration purification on a Superdex 200 10/300 GL column (Table 1).

2.3. Crystallization

Initial crystallization trials were conducted with a Phoenix Liquid Handing System (Art Robbins Instruments) using the Crystal Screen and Index kits from Hampton Research in a 96-well plate format. Crystallization was performed *via* sitting-drop vapour diffusion at 291 K by mixing 150 nl TtFbpA solution (at 20 mg ml^{-1}) with 150 nl well solution. Native TtFbpA crystallized in several conditions and colourless crystals appeared within 2–7 d. The initial hits were optimized using the hanging-drop method by mixing 0.5 µl protein solution at a concentration of 20 mg ml^{-1} with 0.5 µl reservoir solution. The final crystallization condition was 0.2 *M* ammonium acetate, 0.1 *M* sodium acetate trihydrate pH 4.6 and 28%(*w*/*v*) PEG 4000. The

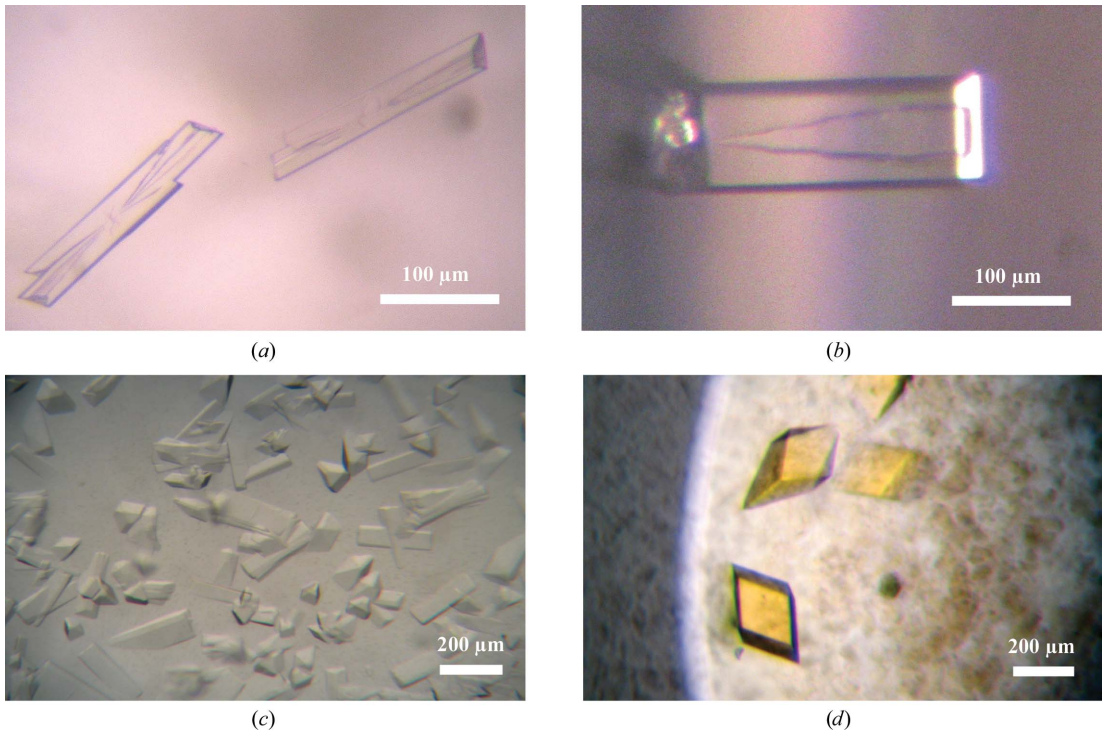

Figure 2
Crystals of TtFbpA. (*a*) Colourless form I. (*b*) Colourless form II. (*c*) Colourless form III. (*d*) Orange form IV.

crystals belonged to the orthorhombic space group $P2_12_12_1$, with unit-cell parameters a = 42.1, b = 139.3, c = 326.5 Å (form I; Fig. 2*a*). Matthews coefficient analysis suggested that five or six monomers of the protein were present in the asymmetric unit (V_M = 2.58 or 2.15 Å^3 Da^{-1}, respectively), with a solvent content of 52.4 or 42.8%, respectively (Matthews, 1968; Kantardjieff & Rupp, 2003).

Crystallization trials for iron-bound TtFbpA were conducted as described previously for native TtFbpA. Several conditions were identified; the crystals in some conditions appeared colourless, while those in others appeared orange. After optimization, colourless crystals grew in 0.2 *M* $LiSO_4$, 0.1 *M* Bis-Tris pH 6.5 and 28%(*w*/*v*) PEG 3350. Initial X-ray analysis revealed that these crystals belonged to the orthorhombic space group $P2_12_12_1$, with unit-cell parameters a = 42.3, b = 139.2, c = 218.9 Å (form II; Fig. 2*b*). Matthews coefficient analysis indicated that either three or four molecules were present in the asymmetric unit (V_M = 2.89 or 2.17 Å^3 Da^{-1}, respectively), with a solvent content of 57.5 or 43.4%, respectively. Another colourless crystal form grew in 0.2 *M* NaCl, 0.1 *M* Bis-Tris pH 5.5 and 25%(*w*/*v*) PEG 3350 and belonged to the monoclinic space group $P2_1$, with unit-cell parameters a = 66.5, b = 61.7, c = 73.9 Å, β = 111.7° (form III; Fig. 2*c*). The asymmetric unit is estimated to contain two molecules, with a corresponding V_M of 1.90 Å^3 Da^{-1} and a solvent content of 35.2%. Orange crystals of TtFbpA containing ferric ions were obtained from drops equilibrated against a reservoir consisting of 0.2 *M* $MgCl_2$, 0.1 *M* HEPES pH 7.5 and 26% PEG 3350 after one week. These crystals belonged to the trigonal space group $P3_121$ or $P3_221$, with unit-cell parameters a = 63.6, b = 63.6, c = 266.7 Å, $\alpha = \beta$ = 90.0, γ = 120.0° (form IV; Fig. 2*d*). The calculated Matthews coefficient was approximately 2.10 Å^3 Da^{-1} assuming the presence of two molecules of TtFbpA in the asymmetric unit, with a solvent content of 41.4%.

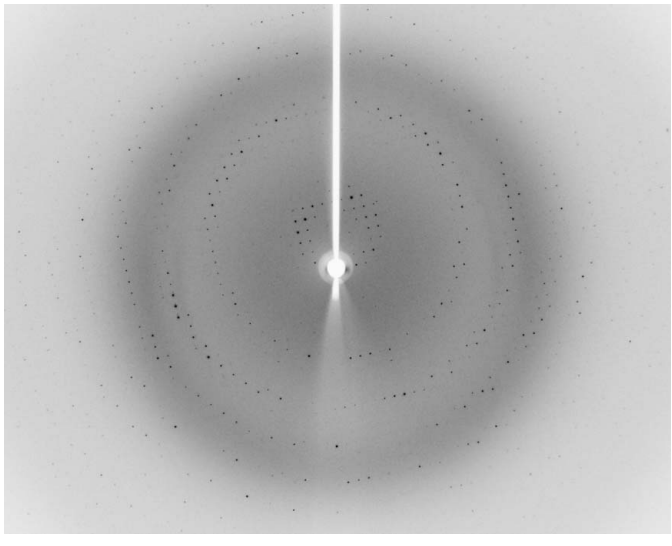

Figure 3
X-ray diffraction pattern from a TtFbpA crystal used to obtain the data in Table 2 for form III. The edge of the detector corresponds to a resolution of 1.90 Å.

2.4. Data collection

Prior to data collection, the crystals were transferred to a cryo-solution consisting of 20% glycerol in mother liquor and flash-cooled in liquid nitrogen. Data collection was performed at 100 K using a wavelength of 0.9791 Å at the BL17U station of the Shanghai synchrotron-radiation source (SSRF) with a MAR 225 CCD detector system (Fig. 3). Initial molecular-replacement trials with available FbpA structures as search models failed to give clear solutions. Therefore, we collected a Br-derivative SAD data set from form I crystals in order to provide experimental phases for structure determination. The form I crystals were soaked in cryoprotectant solution supplemented with 1 *M* sodium bromide and data collection was

Table 2
Data-collection statistics.

Values in parentheses are for the last shell.

	Form I	Form I (Br-derivative SAD data set)	Form II	Form III	Form IV
Wavelength (Å)	0.9791	0.9196	0.9791	0.9791	0.9791
Space group	$P2_12_12_1$	$P2_12_12_1$	$P2_12_12_1$	$P2_1$	$P3_121$ or $P3_221$
Unit-cell parameters					
a (Å)	42.1	41.6	42.3	66.5	63.6
b (Å)	139.3	139.0	139.2	61.7	63.6
c (Å)	326.5	325.2	218.9	73.9	266.7
α (°)	90.0	90.0	90.0	90.0	90.0
β (°)	90.0	90.0	90.0	111.7	90.0
γ (°)	90.0	90.0	90.0	90.0	120.0
Resolution (Å)	50.0–1.91 (1.97–1.91)	50.0–2.40 (2.44–2.40)	50.0–2.07 (2.12–2.07)	40.0–1.90 (1.94–1.90)	50.0–2.50 (2.56–2.50)
Total reflections	1588071	1734705	840378	540412	474240
Unique reflections	143194 (11159)	75082 (3724)	75069 (4618)	44182 (2839)	22650 (1463)
Mean $I/\sigma(I)$	22.0 (7.66)	54.47 (22.58)	15.2 (4.08)	18.4 (2.59)	24.2 (13.7)
$R_{\rm merge}$† (%)	5.8 (15.5)	7.8 (14.5)	7.6 (32.1)	7.9 (45.1)	8.5 (18.0)
Completeness (%)	96.0 (91.9)	99.6 (98.8)	93.4 (86.7)	99.7 (97.3)	99.9 (99.5)
Multiplicity	4.0 (3.6)	11.0 (9.6)	3.4 (3.3)	4.1 (3.5)	6.9 (6.5)

† $R_{\rm merge} = \sum_{hkl}\sum_i |I_i(hkl) - \langle I(hkl)\rangle| / \sum_{hkl}\sum_i I_i(hkl)$, where $I_i(hkl)$ is the ith intensity measurement of reflection hkl, including symmetry-related reflections, and $\langle I(hkl)\rangle$ is its average.

carried out on the SSRF BL17U beamline at the peak wavelength of 0.9196 Å. All data were processed and scaled with the *HKL*-2000 software package (Otwinowski & Minor, 1997). Individual data-processing statistics for the TtFbpA crystals are reported in Table 2.

3. Discussion

During purification, we found that the additive bicarbonate contributed to the orange colour of the TtFbpA sample. This suggests that bicarbonate assists iron binding by TtFbpA, which is consistent with a previous structural study of FbpA from *M. haemolytica* that showed that bicarbonate is involved in binding of ferric ion (Shouldice *et al.*, 2004). However, colourless crystals were also obtained from the crystallization of orange TtFbpA protein solution. We anticipate that these colourless crystals may arise from destabilization of the binding of ferric ions by TtFbpA during crystallization.

We thank Jianhua He, Sheng Huang and Ling Tang at Shanghai Synchrotron Research Facility beamline BL17U for help with data collection. This work was supported by the National Natural Science Foundation of China (Grant No. 31070067) and the Ministry of Education (Grant Nos. 20100002110001 and 20090002120036).

References

Badarau, A., Firbank, S. J., Waldron, K. J., Yanagisawa, S., Robinson, N. J., Banfield, M. J. & Dennison, C. (2008). *J. Biol. Chem.* **283**, 12520–12527.
Berntsson, R. P., Smits, S. H., Schmitt, L., Slotboom, D. J. & Poolman, B. (2010). *FEBS Lett.* **584**, 2606–2617.
Biemans-Oldehinkel, E., Doeven, M. K. & Poolman, B. (2006). *FEBS Lett.* **580**, 1023–1035.
Bruns, C. M., Anderson, D. S., Vaughan, K. G., Williams, P. A., Nowalk, A. J., McRee, D. E. & Mietzner, T. A. (2001). *Biochemistry*, **40**, 15631–15637.
Clarke, T. E., Tari, L. W. & Vogel, H. J. (2001). *Curr. Top. Med. Chem.* **1**, 7–30.
Guo, M., Harvey, I., Yang, W., Coghill, L., Campopiano, D. J., Parkinson, J. A., MacGillivray, R. T., Harris, W. R. & Sadler, P. J. (2003). *J. Biol. Chem.* **278**, 2490–2502.
Higgins, C. F. (1992). *Annu. Rev. Cell Biol.* **8**, 67–113.
Higgins, C. F. (2001). *Res. Microbiol.* **152**, 205–210.
Kantardjieff, K. A. & Rupp, B. (2003). *Protein Sci.* **12**, 1865–1871.
Mao, B., Pear, M. R., McCammon, J. A. & Quiocho, F. A. (1982). *J. Biol. Chem.* **257**, 1131–1133.
Matthews, B. W. (1968). *J. Mol. Biol.* **33**, 491–497.
Otwinowski, Z. & Minor, W. (1997). *Method Enzymol.* **276**, 307–326.
Shouldice, S. R., McRee, D. E., Dougan, D. R., Tari, L. W. & Schryvers, A. B. (2005). *J. Biol. Chem.* **280**, 5820–5827.
Shouldice, S. R., Skene, R. J., Dougan, D. R., Snell, G., McRee, D. E., Schryvers, A. B. & Tari, L. W. (2004). *J. Bacteriol.* **186**, 3903–3910.
Tom-Yew, S. A., Cui, D. T., Bekker, E. G. & Murphy, M. E. (2005). *J. Biol. Chem.* **280**, 9283–9290.